ACS Sustainable Chemistry & Engineering

Research Article

pubs.acs.org/journal/ascecg

Efficiency of Thermally Assisted Capacitive Mixing and Deionization Systems

Daniel Moreno and Marta C. Hatzell*

George W. Woodruff School of Mechanical Engineering, Georgia Institute of Technology, 801 Ferst Drive, Atlanta, Georgia 30309, United States

Supporting Information

ABSTRACT: The temperature of an input solution to an environmental technology can vary greatly depending on numerous industrial and environmental factors. For capacitive mixing (CapMix) and deionization (CDI) based technologies which rely on charge storage within an electric double layer (EDL), this temperature dependence affects energy output and energy consumption. Yet, how temperature-dependent EDL properties impact the thermodynamic efficiency for energy conversion and ion separations is less known. Here, we evaluate how isothermal, nonisothermal and variable temperature profiles impact the thermodynamic efficiency of CDI and CapMix cycles operated under both reversible and irreversible (current dependent) conditions. For CapMix (C_{HC} = 600 mM, C_{LC} = 20 mM, ϕ = 50%), reversible system operation resulted in an optimal efficiency of 43% when $T_{HC} \neq T_{LC}$. For CDI (C_{feed} = 20 mM, $C_{diluate}$ = 5 mM, α = 50%), optimal thermodynamic efficiencies are attained through the use of nonisothermal ($T_{feed} \neq T_{brine}$) or variable temperature operation, and approached 10%. The introduction of current (25 mA) based irreversibilities, however, reduces the maximum attainable CapMix and CDI thermodynamic efficiency to 25% and 3.2% (25 mA).

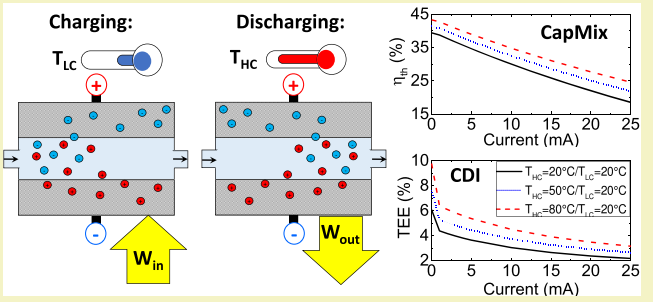

KEYWORDS: *Capacitive deionization, Capacitive mixing, Electric double layer, Thermodynamic efficiency*

INTRODUCTION

Capacitive mixing (CapMix) is a technology which generates energy through controlling spontaneous ionic mixing between two solutions (sea and river water). Conversely, capacitive deionization (CDI) is a technology which consumes energy in order to separate ionic species in a feed stream into two streams (diluate and brine/concentration). Both technologies are electrochemical in nature, and use highly porous supercapacitor based electrodes to generate energy or desalinate water. Thus, optimized ion structuring within the electric double layer (EDL) of a supercapacitor is essential for effective desalination from CDI and energy production from CapMix.[1−5] Extensive investigations have aimed to describe EDL phenomena (desolvation, screening, ion packing) responsible for improving charge storage based processes (electroadsorption/desorption) through theory and experiments.[6−8] Despite these extensive investigations, much of the current focus on charge storage within the EDLs is limited by the assumption that charge storage occurs isothermally.

It is well-known that numerous factors contribute to thermal fluctuations which produce nonisothermal operations. This in turn alters the ion structuring and by extension charge storage dynamics within the EDL.[9,10] Thus, the temperature of a CapMix and CDI cell impacts the system performance (energy consumption, energy generation, thermodynamic efficiency). Within energy storage, thermal properties have been intensely investigated due to the role joule heating plays in materials aging.[1,11−16] Additionally, thermal energy harvesting from EDL capacitors has been suggested through leveraging the thermogalvanic effect.[17,18] The thermogalvanic effect within CapMix systems has been experimentally and theoretically investigated, with performance increasing when the seawater is warm and the river water is cool.[19,20] This improved performance was attributed to a thermally induced double layer expansion process in concert with the concentration induced double layer expansion. This work was also highlighted as a means to reduce energy consumption in CDI cells.[19,21] However, prior computational work has emphasized the importance of infinitely slow cycle operation, where irreversibilities are minimal. Accounting for transients could demonstrate variations with temperature due to effects of resistance and diffusion that had not previously been seen.

Here, we investigate how thermal properties can aid in minimizing electrical energy required for CDI or maximizing electrical energy produced through CapMix. In the first scenario, we examine systems where all four stages of the separations and mixing cycles occur on one isotherm (T = 20−80 °C). Next, we examine the case whereby different cycle

Received: February 12, 2019
Revised: May 25, 2019
Published: June 3, 2019

DOI: 10.1021/acssuschemeng.9b00859
ACS Sustainable Chem. Eng. XXXX, XXX, XXX−XXX

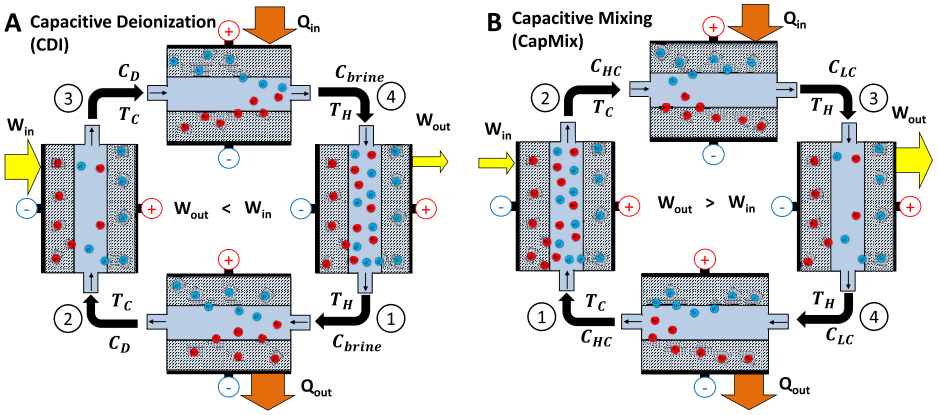

Figure 1. Physical depiction of thermal and electrical energy conversion processes for (a) CDI, and (b) CapMix cycles. Note that both the CapMix and the CDI cycles are operated in a continuous (single-pass) mode during all four stages, and the processes are only depicted in a cyclic manner to demonstrate the energy transfers of work and heat.

stages (charging, discharging, solution switching) are operated on two separate isotherms. Finally, we examine the scenario whereby cycle stages occur with a variable temperature profile (charging, discharging, solution switching). In each case, the desalination and mixing cycle employed is the Carnot-like cycles which operate while maintaining constant chemical potential (iso-μ) during the charging and discharging stages. Each scenario is evaluated in terms of the total electrical energy produced/consumed (CapMix/CDI) and the thermodynamic efficiency.

METHODOLOGY

The investigated CDI cycle consists of four stages and closely resembles experiments where charging and discharging occurs at constant current (Figure 1A). The first stage (process 1-2) consists of a solution switching stage, where the maximum brine concentration is replaced by a minimum diluate concentration. The second stage (process 2-3) consists of a charging stage where the chemical potential was held constant (mimicking a Carnot-like process). The second stage was complete once a maximum set voltage was reached. Stage two represents the desalination process. The third stage (process 3-4) consists of a constant charging phase (no current). This stage is complete once the concentration reaches the predefined brine concentration. The fourth stage (process 4-1) consists of a discharging stage where the chemical potential was held constant (mimicking a Carnot-like process). The fourth stage was complete once a minimum set voltage was reached. Stage four represents the resalination process.

The CapMix cycle consisted of four stages, which also resembled processes employed experimentally. The four stages were similar to those described above. The main difference was that in CapMix charging occurred in the maximum concentration (i.e., seawater, HC) and discharging occurred in the minimum concentration (i.e., river water, LC) (Figure 1B). The cycle started with a maximum concentration (C_{HC}), and the electrodes were held at a constant chemical potential until the cell reached the maximum charging voltage (process 1-2). Then, the solution was switched to the minimum concentration (C_{LC}). This resulted in an increase in the total cell voltage due to the EDL expansion process (process 2-3). Thus, when discharging (process 3-4), the higher voltages enabled net energy recovery. Finally, the high concentration (C_{HC}) was reintroduced during a constant charge switching stage (process 4-1). Note that, in Figure 1, both the CapMix and the CDI cycles are operated in a continuous (single-pass) mode during all four stages, and the processes are only depicted in a cyclic manner to demonstrate the energy transfers of work and heat.

In order to introduce thermal effects into the aforementioned cycles, we investigated three modes of operation. In the first mode, the entire cycle was operated under isothermal conditions (stages 1−4). We investigated cycles operated at (T = 20, 50, 80 °C). In the second mode, we investigated cycles where operations occurred on two isotherms. Specifically, we investigated an operational mode where charging took place at 20 °C, and discharging took place at elevated temperatures (T = 50 and 80 °C). Applying elevated temperatures during the discharging stage was motivated by previous studies.[19,21] In the third mode, we investigate thermal effects in a dynamic matter. Here, we apply a variable temperature profile during the charging phase. The temperature profile applied to the cell was chosen to enable constant chemical potential operation during the charging and discharging stage. As was communicated earlier, constant chemical potential ion separations/mixing in a chemical engine is analogous to the isothermal heat addition process in a heat engine. Furthermore, the use of constant chemical potential separations/mixing has been shown to minimize/maximize the work per number of ions.[19,22]

The simulations were subject to an initial voltage of 0.1 V, and charged at constant concentration until a final voltage of 1.0 V. A maximum of 1.0 V was chosen to mitigate issues associated with electrolysis (e.g., side reactions). Maintaining the discharge voltage at 0.1 V enabled energy recovery during the cycle which is necessary when looking for optimal thermodynamic efficiency in CapMix and CDI systems. For CDI, the maximum (brine) concentration is determined by the C_{feed}, water recovery α, and minimum (dilute) concentration $C_{diluate}$:

$$C_{brine} = \frac{C_{feed} - \alpha C_{diluate}}{1 - \alpha} \quad (1)$$

For CDI cycles, the thermodynamic efficiency (TEE) is the ratio of the Gibbs energy of mixing $\Delta G_{mix,CDI}$ to the input cycle work W_{cycle}, measured by $\oint V\, d\sigma$. To equate units with the Gibbs energy of mixing, σ is represented as a volumetric based charge after dividing by 2× the pore length L_e. The Gibbs energy of mixing and TEE is defined as

$$\Delta G_{mix,CDI} = nRT\left(\frac{C_{feed}}{\alpha}\ln\left(\frac{C_{feed} - \alpha C_{diluate}}{C_{feed}(1-\alpha)}\right) - C_{diluate}\ln\left(\frac{C_{feed} - \alpha C_{diluate}}{C_{diluate}(1-\alpha)}\right)\right) \quad (2)$$

$$TEE = \frac{\Delta G_{mix}}{W_{cycle}} \quad (3)$$

where n is the van 't Hoff Factor, which for 1:1 electrolytes assumes a value of 2. For CapMix, an equivalent efficiency is developed. This thermodynamic efficiency considers the maximum work that can be extracted by the cycle $\Delta G_{mix,CapMix}$:

DOI: 10.1021/acssuschemeng.9b00859
ACS Sustainable Chem. Eng. XXXX, XXX, XXX−XXX

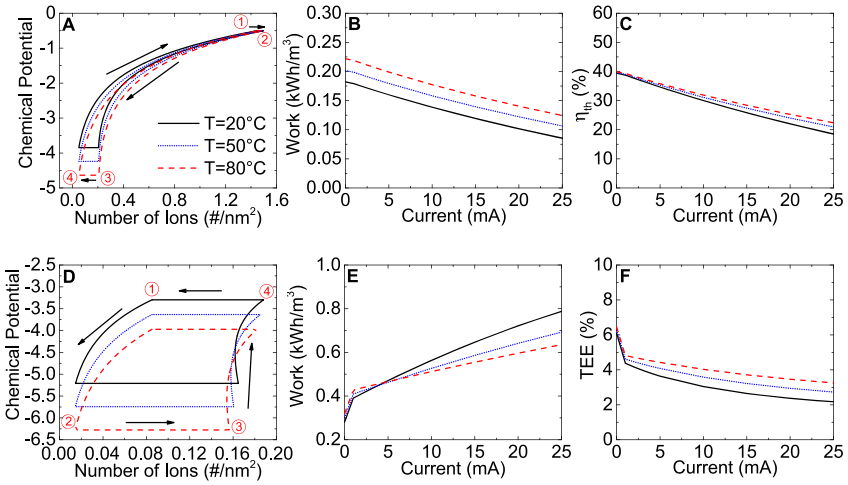

Figure 2. Cycles operated on two isotherms. (A) CapMix $\mu-N$ Diagram, (B) CapMix net-work extracted, and (C) CapMix thermodynamic efficiency. (D) CDI $\mu-N$ Diagram, (E) CDI net-work consumed, and (F) CDI thermodynamic efficiency. Chemical potential is normalized by RT_0, where T_0 represents the dead state temperature.

$$\Delta G_{\mathrm{mix,CapMix}} = -2RT\left(\frac{C_{\mathrm{mix}}}{\phi}\ln\left(\frac{C_{\mathrm{mix}}}{C_{\mathrm{H_2O}}}\right) - (C_{\mathrm{LC}})\ln\left(\frac{C_{\mathrm{LC}}}{C_{\mathrm{H_2O}}}\right) - \frac{1-\phi}{\phi}C_{\mathrm{HC}}\ln\left(\frac{C_{\mathrm{HC}}}{C_{\mathrm{H_2O}}}\right)\right) \quad (4)$$

where ϕ is the volume fraction of low concentration water used during the CapMix process. C_{mix} is the mixture solution, and the volume fraction is fixed at ϕ = 0.5. This indicates that the same amount of water is mixed during both of the switching stages. We have also assumed activity coefficients as unity values. Thus, the thermodynamic efficiency for CapMix is

$$\eta_{\mathrm{th}} = \frac{W_{\mathrm{cycle}}}{\Delta G_{\mathrm{mix,CapMix}}} \quad (5)$$

The detailed development and analysis for ΔG_{mix} at alternating temperatures is discussed in the Supporting Information (Figure SI1).

Chemical potential in chemical systems is the analog to temperature in thermal energy systems, and is represented by

$$\mu = RT\ln\left(\frac{C}{C_{\mathrm{ref}}}\right) \quad (6)$$

where T is temperature, R is the universal gas constant, and C_{ref} represents a reference concentration for the dead/surrounding environment state, taken as 1 M.[23] It can be seen that chemical potential varies as a function of both temperature and concentration. Thus, if the CapMix/CDI cycle operation is isothermal, then a constant concentration process will result in the desired constant chemical potential. If CapMix/CDI cycle operation is nonisothermal, in order to maintain constant chemical potential with variable temperature the concentration must be varied.

We also consider the effects of temperature changes during the charging/discharging stages as well as during switching stages. Here, constant chemical potential is enabled through varying temperature and concentration.[23,24] Operating cycles under variable temperature conditions may provide insight into more realistic means to achieved constant chemical potential operations in experiments. During variable temperature operation, the temperature was limited to 0 to 100 °C.

Changes in the number of ions in the cell (N) are indicated by the following:

$$N = \Gamma + \mathrm{CL_eN_{av}} \quad (7)$$

where Γ is the buildup of ions in the cell from charging, and $\mathrm{CL_eN_{av}}$ is ions directly in the body of the cell (see Supporting Information). When this number of ions in transport is reduced, cycles can operate under conditions closer to Carnot operation.[23] We will explore the ideal steady-state conditions (infinitely slow reversible cycles), then consider the transient mode to simulate more realistic operation.

It is important to note that these reversible cycles are only theoretical, and transient transport limitations still need to be considered. For instance, the infinitely slow model neglects all cell ohmic resistances since current magnitude is assumed negligible. In actuality, the cell exhibits concentration-dependent internal resistances, along with a constant external resistance. The internal resistance within the electrolyte channel is inversely related to the cell conductivity, which depends on both concentration of electrolyte and temperature (Figure SI2A). Additionally, effects of diffusion will also influence transport when current is considered. Temperature strongly influences diffusion (Figure SI2B) due to the increase in thermal vibrations within the electrolyte at higher temperatures, which can further aid in effective ion transport. For all other important operational parameters for the transient analysis, such as properties and geometries, see Table SI1.

RESULTS AND DISCUSSION

CDI and CapMix Cycles Operated with Isothermal Input Streams. To evaluate the effect input solution temperature has on system level performance (energy production, consumption, and thermodynamic efficiency), we initially investigated CDI and CapMix cycles which occur under infinitely slow conditions. Through neglecting kinetic effects, we can evaluate the impact of solution temperature under theoretically ideal (reversible) system operation (Figure 2A). For CapMix operation, the high concentration (C_{HC}) is 600 mM, the low concentration (C_{LC}) is 20 mM, and the volume ratio is fixed at ϕ = 50%. For CDI, the inlet feed concentration is 20 mM (C_{feed}), the diluate concentration is 5 mM (C_{diluate}), and the water recovery is fixed at α = 50%. The voltage limit in all cases is 0.1 to 1 V. We also expand the GCS CDI model to evaluate kinetic and ohmic based irreversibilites (Figure 2B,C).

During the reversible and isothermal CapMix cycles, increasing the cell temperature (from 20 to 80 °C) results in a decrease in the accumulated surface charge (from 0.24 to 0.22 #/nm^2) at fixed voltage (V = 1 V). Despite this slight reduction in the maximum charge obtained, the cell discharge

DOI: 10.1021/acssuschemeng.9b00859
ACS Sustainable Chem. Eng. XXXX, XXX, XXX−XXX

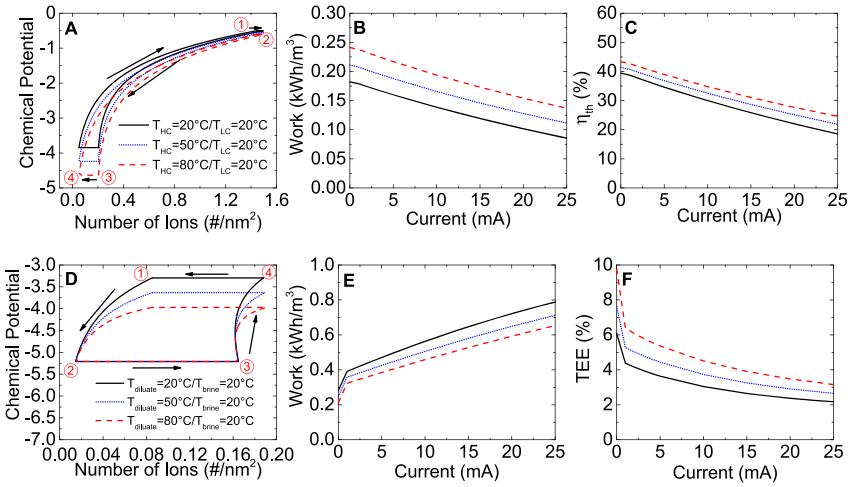

Figure 3. Cycles operated on two isotherms. (A) CapMix $\mu-N$ Diagram, (B) CapMix net-work extracted, and (C) CapMix thermodynamic efficiency. (D) CDI $\mu-N$ Diagram, (E) CDI net-work consumed, and (F) CDI thermodynamic efficiency. Chemical potential is normalized by RT_0, where T_0 represents the dead state temperature.

voltage rises due to a 5 mV jump in the thermal voltage from 20 to 80 °C. As a result, the net-work extracted from the CapMix cycle increases from 0.18 to 0.27 kWh per m^3 of solution mixed, as temperature increases from 20 to 80 °C. Graphically, the greater electrical energy generation is represented by an increase in the area of the chemical potential−number of ions ($\mu-N$) diagram (Figure 2A) and charge−voltage ($\sigma-V$) diagrams (Figure SI3A). Thus, the increase in net-work equates to 1.0 Wh per m^3 per °C of mixed solution. The theoretical cycle thermodynamic efficiency also increased from 39 to 43%. We note that reversible net-work and thermodynamic efficiency correspond to a cell operated at zero current(Figure 2B,C).

During the reversible and isothermal CDI cycles, increasing the cell temperature (from 20 to 80 °C) again results in an increase in the surface charge during charging (from 0.19 to 0.21 #/nm^2) at fixed voltage (V = 1 V). Again, the increase in surface charge results in an increase in net-work, indicated by the larger area on both $\mu-N$ (Figure 2D) and $V-\sigma$ diagrams (Figure SI3B). However, this net-work is consumed by the cell, rather than produced. Thus, the work input for the same separations increased from 0.28 to 0.32 kWh per m^3 of solution separated, as the solution temperature increased from 20 to 80 °C (Figure 2E). This results in an increase energy which corresponds to 0.65 Wh per m^3 per °C. Despite the increase in energy consumed for the separation process, higher temperatures also increase the Gibbs energy of mixing. As a result, the cycle thermodynamic efficiency actually increased slightly from 6.1 and 6.4% as the cell temperature increased to 80 °C (Figure 2F, current = 0 mA).

When the CDI and CapMix cycles are operated irreversibly, the performance (net-work and thermodynamic efficiency) is dependent on the cell operating current. Ideally, CapMix cycles need to operate under conditions which minimize resistive losses. When comparing irreversible cycles directly with reversible cycles, a voltage discontinuity exists during solution switching (Figure SI4A−C). This abrupt transition increases the cell voltage due to changes in the structure of the EDL (Debye Length). As the switching stage proceeds the voltage spike decreases as the effluent cell concentration approaches that of the recently introduced diluate stream. This spike has been observed experimentally.[4,24] As the operating current increases, the net-work generated from the mixing process decreases due to resistance based irreversibilities. Nevertheless, at all current values, the net-work for CapMix increases with temperature. At the maximum value of 25 mA, the net-work output was 0.09, 0.11, and 0.12 kWh per m^3 for 20, 50, and 80 °C. This corresponded to thermodynamic efficiency values of 19, 21, and 22% (Figure 2C). We attribute the increase in the η_{th} with temperature due to the gradually nonlinear increase in the net cycle work output (Figure SI5).

For irreversible CDI cycles, higher temperature increased the work required up to a 3−5 mA threshold; however, the thermodynamic efficiency also increased with temperature (Figure 2E and F). Increasing current decreased the maximum attainable thermodynamic efficiency due to a greater amount of irreversibilities (ohmic resistance) present at high current. Therefore, while increasing the temperature during isothermal operation does augmented system performance for CapMix (increased energy recovery), it degraded system performance for CDI (increased energy consumed). This indicates that if system operation is to occur at a fixed temperature with minimal charging current, elevated temperatures are preferred for CapMix whereas low temperatures are preferred for CDI.

CDI and CapMix Cycles Operated with Nonisothermal Input Streams. In addition to cycles operated isothermally, cycles whereby individual processes occur at different or varying temperatures are possible. Here, we investigate cycles where charging occurs on one isotherm, and discharging occurs on a second isotherm. Practically speaking, this is relevant in cases where the inputs (C_{feed}, C_{brine}, C_{HC}, C_{LC}) are sent through a heat exchanger prior to the CDI or CapMix system. Additionally, the individual input streams may originate at different temperatures due to industrial or environmental setting. As outlined for cycles operated on a single isotherm, we evaluate the cycle performance in terms of the energy production/consumption and thermodynamic efficiency. For both CapMix and CDI, we employ the same voltage, concentration, and operating conditions described above. In addition, we performed simulations which mimicked reversible (Figure 3A) and irreversible system operation (Figure 3B,C).

For CapMix cycles, isothermal charging of the cell occurred at 20 °C, and isothermal discharging now occurred at 20, 50,

DOI: 10.1021/acssuschemeng.9b00859
ACS Sustainable Chem. Eng. XXXX, XXX, XXX−XXX

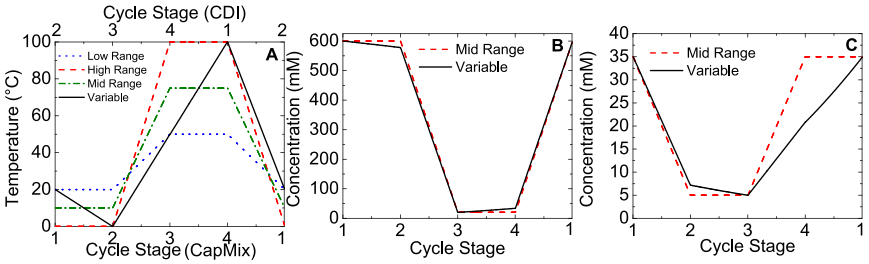

Figure 4. (A) Variable temperature profiles applied to CDI/CapMix cycles. Resulting concentration profiles for (B) CapMix and (C) CDI cycle.

and 80 °C. Since charging temperature is held constant, surface charge remains constant during the charging phase. For the reversible case, the net-work output was 0.18, 0.21, and 0.24 kWh per m^3 of solution mixed, for isothermal discharging at 20, 50, and 80 °C. This resulted in a cycle thermodynamic efficiency of 39%, 41%, and 43% (Figure 3B). This change is only marginally noticeable on a $\mu-N$ diagram (Figure 3A), as a fixed chemical potential during charging limits the swept area. However, the $\sigma-V$ plot clearly delineates the increase in the cell discharge voltage (Figure SI3C), increasing the area for the output work. Thus, the net-work improved by 10% when the cycle was operated between the two isotherms (T_{HC} = 20 and T_{LC} = 80 °C) when compared with isothermal operation at 20 °C. The maximum cycle net work improved by 9% when only the discharging stage operated at elevated temperatures, indicating the benefit of maintaining the low temperature during the charging stage.

For reversible CDI cycles, increasing the temperature during the discharging stage reduced the cycle net-work. The energy consumption was 0.28, 0.24, and 0.21 kWh per m^3 of solution separated, for isothermal discharging at 20, 50, and 80 °C. This resulted in a thermodynamic efficiency of 6.1, 7.6, and 9.8% (Figure 3E, current = 0 mA) for temperatures of 20, 50, and 80 °C. Thus, the net-work decreased by 25% when the cycle was operated between the two isotherms (T_{HC} = 20 and T_{LC} = 80 °C) when compared isothermal operation at 20 °C. In addition, the net-work was 34% less than isothermal testing conducted at 80 °C, indicating that operating between two isotherms is preferable for CDI.

Irreversible CapMix cycles operated on two isotherms displayed similar trends to CapMix operated on one isotherm. Specifically, increasing current decreased net-work from CapMix (Figure 3B). This is anticipated due to ohmic and kinetic based irreversibilities. The net-work output, however, increased with increasing discharge temperature. Opposite to the isothermal case, the net-work consumed for CDI decreased with increasing discharge temperature. In addition, thermodynamic efficiency decreased with current and increased with temperature (Figure 3C−F).

CDI and CapMix Cycles Operated with Input Streams with Varying Temperatures. Finally, for both CapMix and CDI cycles, we consider the performance of a cycle where charging and discharging occur with a variable temperature profile. Like the previously investigated cycles, charging and discharging occurs while chemical potential is fixed (iso-μ), resembling the Carnot-like ion separations/mixing.[25] However, in order to maintain a constant chemical potential while temperature is varied, here the concentration profile must also vary (eq 6). Note that the cycle also maintains a constant number of ions (iso-N) during solution switching.

For the CapMix system, we start by charging (process 1-2) at room temperature (20 °C), and cool the stream to a minimum temperature of 0 °C (Figure 4A, black line). During the switching stage (process 2-3), the cell is gradually heated to a temperature of 50 °C. During the discharging stage (process 3−4), the cell will continue to be gradually heated to a maximum temperature of 100 °C. Finally, in the switching stage (process 4-1), the reactor is cooled and returns to the temperature of 20 °C. Note that this operation is both a cycle with respect to the chemical engine, and with respect to the heat engine. The temperature profiles described and graphically shown in Figure 4 are the same for the CDI cell; however, the stages are different (Figure 4, top x-axis).

To compare this unique mode of temperature based operation illustratively, three alternative cases are considered in which temperature changes occur in the switching stage only while the charge/discharge processes are isothermal (Figure 4A). The lowest temperature range assumes that T_{charge} = 20 °C and $T_{discharge}$ = 50 °C (ΔT = 30 °C, T_{avg} = 35 °C). The high range assumes the T_{charge} = 0 °C and $T_{discharge}$ = 100 °C (ΔT = 100 °C and T_{avg} = 50 °C). A third case considers the averaged temperatures between the high range and low range T_{charge} = 75 °C, $T_{discharge}$ = 10 °C (ΔT = 65 °C and T_{avg} = 42.5 °C).

For the mid range, we show the corresponding cycle variations in concentration, which also coincides with the high and low temperature ranges. When the variable temperature cycle is compared to the cycles with temperature changes in the switch stage only, concentration changes in the CapMix cycles vary only by up to 25 mM, or 5% of C_{HC} (Figure 4B). The switching stage only requires recovery to the initial concentration, and during discharging, the concentration is returned to brine (Figure 4C). For these iso-chemical potential studies, we only consider the reversible cycle.

The quantitative effect of the variable temperature based operation is illustrated on $\sigma-V$ and $\mu-N$ diagrams. For CapMix, the variable temperature does not increase the cycle output work (Figure 5A,B). For each of the cycles studied, the overall cycle work is 0.21 kWh/m^3 for the low range, 0.27 kWh/m^3 for the high range, 0.24 kWh/m^3 for the mid range, and 0.21 kWh/m^3 for the variable temperature. Subsequently, the efficiencies for each of the cycles are 41.4% (low range), 43.5% (high range), 45.6% (mid range), and 41.3% (variable temperature). Additionally, the work output per number of ions exchanged values were 0.15 (low range), 0.19 (high range), 0.17 (mid range), and 0.15 (variable temperature) kWh/m^3/#/nm^2. Thus, for CapMix, maximizing the temperature range between charge and discharge improved performance, while employing variable temperatures offered minimal overall benefit for the cycle. This is despite the fact that the variable temperature is more Carnot-like.

DOI: 10.1021/acssuschemeng.9b00859
ACS Sustainable Chem. Eng. XXXX, XXX, XXX−XXX

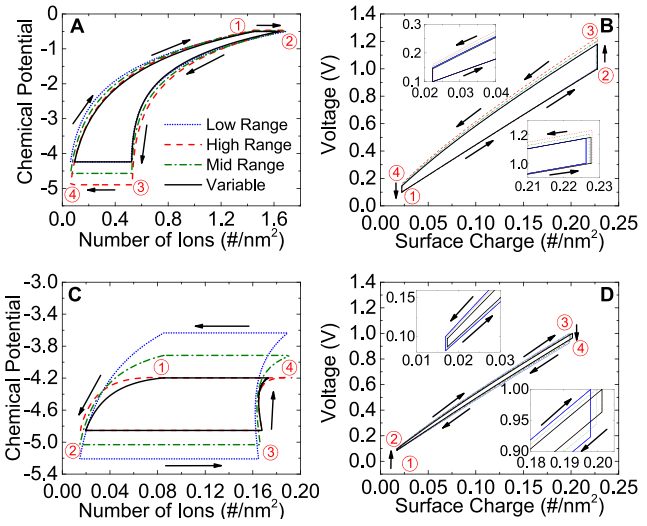

Figure 5. Variable temperature profile operation (A) $\mu-N$ diagram for CapMix, (B) $\sigma-V$ diagram for CapMix, (C) $\mu-N$ diagram for CDI, (D) $\sigma-V$ diagram for CDI.

For CDI, the variable temperature did aid in decreasing the net-work consumed by the cycle (Figure 5C,D). The cycle net-work is only 0.14 kWh/m^3 for the variable cycle operation, whereas the temperature-averaged mid range was 0.20 kWh/m^3, the maximum temperature range 0.15 kWh/m^3, and the low range 0.20 kWh/m^3. The cycle TEE comparison follows with values of 7.6%, 14.9%, 10.3%, and 10.0% for the tested temperature ranges of low, high, mid, and variable. Furthermore, the range in the number of ions was the smallest (0.15 #/nm^2) for the variable range of all cycles (Figure 5C). With 0.17, 0.18, and 0.18 #/nm^2 reported for the cycles operated with a high, low, and mid temperature ranges. The nearly 0.02 #/nm^2 over the cycle may appear small, but is a nearly 15% reduction in total the number of ions. Furthermore, the change in number of ions during this switching process is nearly four times less than those of all of the other temperature cases, suggesting that the variable temperature operation may be valuable in future applications for simulating Carnot conditions experimentally. While savings do exist from operating at elevated temperatures, the energy benefits are small compared to the quantity of the thermal energy input to the system (Tables SI2 and SI3). Thus, increased temperature during isothermal processes must be achieved through waste-heat. The maximum energy savings relative to the maximum theoretical Carnot cycle efficiency is 2.37%, which occurs for irreversible cycles at 50 °C and 25 mA (Table SI3).

CONCLUSIONS

We show how tuning the temperature of the input solutions to a CapMix and CDI system can enhance system performance (energy production, energy consumed, and thermodynamic efficiency). When operating CapMix and CDI isothermally, increasing the operating temperature aids in maximizing the net-work output from the CapMix system by up to 50%. Conversely, increasing the operating temperatures has an adverse effect on CDI operation, increasing energy consumption by ∼15%. Additional cycles whereby input solution temperature is individually varied (e.g., $T_{HC} \neq T_{LC}$ and $T_{diluate} \neq T_{brine}$), resulted in enhanced CDI performance. However, CapMix performance never exceeded that attained under high temperatures with isothermal ($T_{HC} = T_{LC} = T_{high\ temp}$). Specifically, by charging in a low temperature feed, and discharging in a high temperature brine, we show that thermodynamic efficiencies can exceed 9%. This is in contrast to isothermal operation which only obtains maximum thermodynamic efficiencies of ∼6%. We note that thermodynamic efficiency, in addition to being dependent on temperature, is also dependent on the feed concentration and percent of salt removed. Finally, a variable temperature profile is explored as a means to operate a CDI and CapMix cycle with Carnot-like electrosorption behavior (iso-μ). Again, performance improvements did not result in benefits for CapMix, but CDI performance increased with temperature up to almost 10% for the conditions tested. Ion mixing and separation based technologies provide new approaches toward harvesting energy and performing ionic separations using only electrical energy input. However, system performance improvements must occur in order for implementation to take place. Through gaining an understanding regarding the role various system level properties play, one can begin to design system level operational modes which most closely mimic theoretical optimal performance.

ASSOCIATED CONTENT

Supporting Information

The Supporting Information is available free of charge on the ACS Publications website at DOI: 10.1021/acssuschemeng.9b00859.

Additional calculations, derivations, and parameters derived from experiments (PDF)

AUTHOR INFORMATION

Corresponding Author

*M. C. Hatzell. E-mail: marta.hatzell@me.gatech.edu. Phone: +1 404-385-4503.

ORCID

Marta C. Hatzell: 0000-0002-5144-4969

Notes

The authors declare no competing financial interest.

ACKNOWLEDGMENTS

This material is based upon work supported by the National Science Foundation under Grant No. (1706290). This work is also supported by the ARCS graduate fellowship to Daniel Moreno.

REFERENCES

(1) Miller, J. R.; Simon, P. Electrochemical capacitors for energy management. *Science* **2008**, *321*, 651−652.

(2) Biesheuvel, P. M. Thermodynamic cycle analysis for capacitive deionization. *J. Colloid Interface Sci.* **2009**, *332*, 258−264.

(3) Biesheuvel, P. M.; Bazant, M. Z.; Cusick, R. D.; Hatton, T. A.; Hatzell, K. B.; Hatzell, M. C.; Liang, P.; Lin, S.; Porada, S.; Santiago, J. G.; Smith, K. C.; Stadermann, M.; Su, X.; Sun, X.; Waite, T. D.; van der Wal, A.; Yoon, J.; Zhao, R.; Zou, L.; Suss, M. E. Capacitive Deionization−defining a class of desalination technologies. *arXiv* **2017**, 1709.05925.

(4) Brogioli, D.; Ziano, R.; Rica, R.; Salerno, D.; Mantegazza, F. Capacitive mixing for the extraction of energy from salinity differences: survey of experimental results and electrochemical models. *J. Colloid Interface Sci.* **2013**, *407*, 457−466.

(5) Moreno, D.; Bootwala, Y.; Tsai, W.-Y.; Gao, Q.; Shen, F.; Balke, N.; Hatzell, K. B.; Hatzell, M. C. In Situ Electrochemical Dilatometry

DOI: 10.1021/acssuschemeng.9b00859
ACS Sustainable Chem. Eng. XXXX, XXX, XXX−XXX

of Phosphate Anion Electrosorption. *Environ. Sci. Technol. Lett.* **2018**, *5*, 745−749.
(6) Bazant, M. Z.; Thornton, K.; Ajdari, A. Diffuse-charge dynamics in electrochemical systems. *Phys. Rev. E: Stat. Nonlinear Soft Matter Phys.* **2004**, *70*, 021506.
(7) Moreno, D.; Hatzell, M. The influence of feed-electrode concentration differences in flow-electrode systems for capacitive deionization. *Ind. Eng. Chem. Res.* **2018**, *57*, 8802−8809.
(8) Moreno, D.; Hatzell, M. Efficiency of Carnot and Conventional Capacitive Deionization Cycles. *J. Phys. Chem. C* **2018**, *122*, 22480−22486.
(9) d'Entremont, A.; Pilon, L. Scaling laws for heat generation and temperature oscillations in EDLCs under galvanostatic cycling. *Int. J. Heat Mass Transfer* **2014**, *75*, 637−649.
(10) d'Entremont, A.; Pilon, L. First-principles thermal modeling of electric double layer capacitors under constant-current cycling. *J. Power Sources* **2014**, *246*, 887−898.
(11) Gualous, H.; Louahlia-Gualous, H.; Gallay, R.; Miraoui, A. Supercapacitor thermal modeling and characterization in transient state for industrial applications. *IEEE Trans. Ind. Appl.* **2009**, *45*, 1035−1044.
(12) Rafik, F.; Gualous, H.; Gallay, R.; Crausaz, A.; Berthon, A. Frequency, thermal and voltage supercapacitor characterization and modeling. *J. Power Sources* **2007**, *165*, 928−934.
(13) Schiffer, J.; Linzen, D.; Sauer, D. U. Heat generation in double layer capacitors. *J. Power Sources* **2006**, *160*, 765−772.
(14) d'Entremont, A. L.; Girard, H.-L.; Wang, H.; Pilon, L. Electrochemical transport phenomena in hybrid pseudocapacitors under galvanostatic cycling. *J. Electrochem. Soc.* **2016**, *163*, A229−A243.
(15) d'Entremont, A. L.; Pilon, L. Thermal effects of asymmetric electrolytes in electric double layer capacitors. *J. Power Sources* **2015**, *273*, 196−209.
(16) Guillemet, P.; Scudeller, Y.; Brousse, T. Multi-level reduced-order thermal modeling of electrochemical capacitors. *J. Power Sources* **2006**, *157*, 630−640.
(17) Sales, B. B.; Burheim, O. S.; Porada, S.; Presser, V.; Buisman, C. J.; Hamelers, H. V. Extraction of energy from small thermal differences near room temperature using capacitive membrane technology. *Environ. Sci. Technol. Lett.* **2014**, *1*, 356−360.
(18) Härtel, A.; Janssen, M.; Weingarth, D.; Presser, V.; van Roij, R. Heat-to-current conversion of low-grade heat from a thermocapacitive cycle by supercapacitors. *Energy Environ. Sci.* **2015**, *8*, 2396−2401.
(19) Janssen, M.; Härtel, A.; Van Roij, R. Boosting capacitive blue-energy and desalination devices with waste heat. *Phys. Rev. Lett.* **2014**, *113*, 268501.
(20) Ahualli, S.; Fernández, M. M.; Iglesias, G.; Delgado, Á. V.; Jiménez, M. L. Temperature effects on energy production by salinity exchange. *Environ. Sci. Technol.* **2014**, *48*, 12378−12385.
(21) Zhang, J.; Hatzell, K. B.; Hatzell, M. C. A Combined Heat-and Power-Driven Membrane Capacitive Deionization System. *Environ. Sci. Technol. Lett.* **2017**, *4*, 470−474.
(22) Boon, N.; Van Roij, R. Blue energy from ion adsorption and electrode charging in sea and river water. *Mol. Phys.* **2011**, *109*, 1229−1241.
(23) Boon, N.; van Roij, R. 'Blue energy' from ion adsorption and electrode charging in sea and river water. *Mol. Phys.* **2011**, *109*, 1229−1241.
(24) Rica, R. A.; Brogioli, D.; Ziano, R.; Salerno, D.; Mantegazza, F. Ions transport and adsorption mechanisms in porous electrodes during capacitive-mixing double layer expansion (CDLE). *J. Phys. Chem. C* **2012**, *116*, 16934−16938.
(25) Boon, N.; Van Roij, R. "Blue energy" from ion adsorption and electrode charging in sea and river water. *Mol. Phys.* **2011**, *109*, 1229−1241.

DOI: 10.1021/acssuschemeng.9b00859
ACS Sustainable Chem. Eng. XXXX, XXX, XXX−XXX